Assessing the Effects of Different Process Parameters on the Pyrolysis Behaviors and Thermal Dynamics of Corncob Fractions

Xiwen Yao,[a] Kaili Xu,[a,*] and Yu Liang [b]

The influence of heating rate, gas flow, and biomass particle size on the pyrolysis and thermal dynamics of corncobs (CC) was investigated experimentally using the quantitative method of thermogravimetric analysis (TGA) coupled with mass spectrometry (MS), and the obtained results were compared in depth. For the examined heating rates of 5, 10, and 20 °C/min, the CC pyrolysis at higher heating rates resulted in a more complete decomposition. The initial pyrolysis temperature decreased when gas flow was increased from 30 to 90 mL/min, whereas the weight loss increased. Particle sizes ($d \leq 74$ μm, 74 μm < $d \leq 154$ μm, 154 μm < $d \leq 280$ μm, and 280 μm < $d \leq 450$ μm) had pronounced effects on the thermal decomposition and bio-syngas compounds (CO, CO_2, CH_4, and H_2) distribution. The emission intensities of most the gaseous products increased at the elevated heating rate, while they decreased with increasing gas flow. In sum, the pyrolysis of CC particles of 154 μm < d ≤ 280 μm under 20 °C/min and in a gas flow of 30 to 60 mL/min was the most appropriate for bio-syngas production in industrial applications.

Keywords: Corncob; Pyrolysis; Heating rate; Gas Flow; Particle Size; Thermal Dynamics; Bio-syngas

*Contact information: a: School of Resources and Civil Engineering, Northeastern University, Shenyang 110819, PR China; b: College of Information Science and Engineering, Northeastern University, Shenyang 110819, PR China; *Corresponding author: neu_kailixu@126.com*

INTRODUCTION

Considering the depletion of fossil fuel sources and the high sensitivity of the public toward environment protection from the conventional energetic systems, the exploration of alternative and renewable energy sources has attracted increasing attention (Shen *et al*. 2013). As an alternative to fossil fuels, biomass, such as agricultural and wood wastes, has become one of the most significant elements of the sustainable energy system due to its abundance, renewability, and environmental benefits (Czernik and Bridgwater 2004). Biomass pyrolysis, as the key sub-category process of biomass thermo-chemical conversion, converts biomass waste in the absence of oxygen to obtain an array of gaseous, liquid, and solid products (Mohan *et al*. 2006; Lv *et al*. 2012), which can be further used to produce fuels, chemicals, heat, and electricity (Meng *et al*. 2013).

The technique of thermogravimetric analysis (TGA) and differential scanning calorimetry (DSC) coupled with mass spectrometry (MS) has become more important for studying the weight loss characteristics, thermal stability, gas products distribution, and the correlation between pyrolysis reactions and chemical structure in biomass (Singh *et al*. 2012; Alshehri *et al*. 2013; Wang *et al*. 2014). The characteristic parameters of the thermal pyrolysis can be obtained from the thermogravimetric (TG) and differential

thermogravimetric (DTG) data during the TGA experiments to further investigate the thermal degradation mechanism (Gai *et al*. 2013).

The pyrolysis behaviors of a variety of agricultural wastes, such as apple pomace (Baray *et al*. 2014), hardwood residues (Mazlan *et al*. 2015), corn stalk (Pittman *et al*. 2012), peanut shells (Yao *et al*. 2016a), grape residues (Xu *et al*. 2009), rice husk and straw (Worasuwannarak *et al*. 2007), wheat and corn straw (Lanzetta and Di Blasi 1998), and cherry seeds (Duman *et al*. 2011), have been investigated for different purposes. Miura and Maki (1998) and Arora *et al.* (2009) have focused on developing mathematical dynamic models for predicting the pyrolysis characteristics of various biomass wastes. In these studies, the chemical composition and pyrolysis behavior of different biomass fractions were greatly different from each other. In the present research, corncobs (CC) waste was chosen as the source of renewable energy due to its abundant availability in China and good potential to produce high value-added products (Yao *et al*. 2016b).

Biomass pyrolysis is an extremely complex process that involves complicated chemical processes and complex physical processes such as mass transfer, heat transfer, and their interactions (Lv *et al*. 2012; Gai *et al*. 2013). There have been many studies on the pyrolysis of CC (Cao *et al*. 2004; Feng *et al*. 2006; Ates and Isikdag 2009; Ioannidou *et al*. 2009; Zhang *et al*. 2009; Trninic *et al*. 2012; Liu *et al*. 2014). Most of these studies focused on developing kinetics models to predict the weight loss characteristics of CC and the reaction dynamics, and only a few were concentrated on the emission regularities of bio-syngas products (consisting primarily of CO, CO_2, CH_4, and H_2) during the pyrolysis as well as on the key factors affecting the thermal degradation.

Furthermore, the pyrolysis of CC remains uncertain in many details, especially in terms of heat and mass transfer, thermal dynamics, and gas products distribution affected by different thermolysis conditions, biomass particle size, and indirectly, the catalytic effects. In general, biomass composition is one of the most significant factors affecting the pyrolysis of biomass, which is composed of cellulose, hemicellulose, and lignin (Ates and Isikdag 2009). According to Meng *et al*. (2013), the pyrolysis of biomass involves the superposition of the pyrolysis of these three biomass components, and it can be also strongly influenced by the experimental conditions.

Therefore, elucidating the influence of different reaction parameters (heating rate, the pyrolysis temperature, the carrier gas, and the pyrolysis medium, *etc*.) together with many other factors (biomass feed particle size and the catalyst, *etc*.) on the pyrolysis of CC fractions is essential for a better understanding of their thermochemical conversion. In this study, the influence of heating rate, gas flow, and biomass particle size on the thermal degradation, heat transfer, kinetics information and organic reaction mechanisms in chemistry, and releasing characteristics of bio-syngas products during the pyrolysis of CC was investigated using the quantitative method of TGA-DSC-MS.

In general, TGA analysis is very useful in determining the preliminary kinetics of biomass pyrolysis. It has been used extensively for the characterization of various feedstock. But, there is a lack of kinetics information on the thermal pyrolysis of CC. Besides, the organic reaction mechanisms in chemistry during the pyrolysis process is also unclear. Therefore, conducting a comprehensive investigation on the pyrolysis of CC is very essential, and the objectives of this study are to obtain the characterization of CC related to thermo-chemical conversions, and to analyze the effects of different process parameters on the kinetics information of CC as well as the organic reaction mechanisms in chemistry. This study can provide a more integrated understanding of the complete pyrolytic process of CC fractions.

EXPERIMENTAL

Preparation of Materials and Characterization

The CC biomass samples were collected from the countryside of Shenyang, northeast China. The raw biomass samples were oven-dried at 105 °C ± 0.5 °C for 24 h, ground and pulverized using a high-speed rotary cutting mill, and sieved with a 100-mesh sieve (0.154 mm in size). The materials that passed through the sieve and those not passed through the sieve were gathered in two different closed containers and kept for analysis. The proximate, ultimate, and component analyses of those CC materials are listed in Table 1, with each value being the mean value of three tests.

The proximate analysis was conducted on an as-received basis, while ultimate analysis and low heating value (LHV) was performed on a dry basis. The volatile matter, fixed carbon, and ash content were measured by 5E-MACIII Infrared Speediness Coal Analyzer (Kaiyuan Co., Changsha, China). The moisture was determined by a Sartorius Moisture Analyzer IMA 30 (Hamburg, Germany). Ultimate analysis was performed on a Vario MACRO Elemental Analyzer (Elementar, Hanau, Germany). The LHV of CC fractions was measured by IKA Calorimeter System C2000 (IKA Co., Staufen, Germany). The proximate and ultimate analyses, and the chemical components of the CC fractions were analyzed according to GB/T 28731-2012 (2012) and ASTM E1758-01 (2015), respectively. All the values in Table 1 presented a good reproducibility with a relative standard deviation less than 2.0%, and the precision of these measurements was 0.5%.

Table 1. Proximate, Ultimate, and Component Analyses of CC Samples

Proximate Analysis (wt.%)		Ultimate Analysis (wt.%)		Chemical Components (wt.%)	
Moisture	0.87	C	47.26	Cellulose	47.60 ± 3
Volatiles	79.25	H	5.79	Lignin	16.40 ± 0.6
Ash	2.24	O	43.23		
Fixed Carbon	17.64	N	0.56	Hemicellulose	32.00 ± 2
Low Heating Value (MJ/kg)	18.15	S	0.05		

TGA-MS Experiments and Quantitative Method

The TGA tests of those prepared CC samples (less than 0.154 mm in size) were performed in a sensitive thermal balance (NETZCH-STA449 F3, Selb, Germany) at the heating rates of 5, 10, and 20 °C/min with a gas flow of 10 mL/min from 25 °C up to a final temperature of 1200 °C. For determining the influence of gas flow on the pyrolysis prepared CC samples, high purity helium (99.99%) in the gas flow of 30, 60, and 90 mL/min at the heating rate of 30 °C/min was used as the carrier gas. To study the effects of biomass particle size on the thermal degradation and gas products distribution in the pyrolysis, the pyrolysis behaviors of CC fractions of varying diameter ($d \leq 74$ μm, 74 μm $< d \leq 154$ μm, 154 μm $< d \leq 280$ μm, and 280 μm $< d \leq 450$ μm) at the heating rate of 20 °C/min with a gas flow of 30 mL/min were compared.

The sensitivity of this thermal balance was 1 μg and 0.01 °C, and the CC samples needed for each test were about 5 mg. To guarantee the accuracy of pyrolysis experiments and minimize the errors, the best particles sizes for TGA experiments using this thermal balance should be not more than 0.50 mm. Here, the pretreated CC fractions that passed through a 100-mesh (0.154 mm) sieve were further sieved using a 200-mesh

(0.074 mm) screen, and thus both the particles of $d \leq 74$ μm and those of 74 μm < $d \leq$ 154 μm were obtained. Similarly, the CC particles that had not passed through the 100-mesh screen, namely particles of $d > 154$ μm, were further sieved by a 60-mesh (0.28 mm) sieve, and then sieved by a 40-mesh (0.45 mm) sieve, and thus the CC particles of 154 μm < $d \leq 280$ μm and 280 μm < $d \leq 450$ μm were obtained sequentially.

The MS measurements were carried out by a quadrupole MS spectrometer (QMS 403D, Pfeiffer Vacuum Technology, Selb, Germany) coupled to the thermal balance to measure typical gas products. The MS spectrometer was performed in the EI mode with 70 eV of electron energy. To avoid secondary reactions, the gases released were purged to the MS spectrometer immediately to obtain gas evolution curves. The transfer line and gas cell were preheated to 200 °C to avoid cold spots and to prevent the condensation of semi-volatile products. A quantitative method on the MS was implemented by calibration for the following species: CO, CO_2, CH_4, and H_2, based on the quantitative analysis on signals for their mass numbers. Details of this method can be found in a previous paper (Yao *et al*. 2016a). The calibration is taken on the MS spectrometer directly to obtain the method file before the measurement.

Thermal Dynamic Analysis

Thermal dynamic parameters were determined by the integral Coats-Redfern method, which has been successfully employed to investigate biomass pyrolysis kinetics (Vamvuka *et al*. 2003; Sun *et al*. 2010). The global kinetics of the biomass pyrolysis based on the first-order-reaction can be expressed as follows (Rath and Staudinger 2001),

$$k = A\exp\left(-\frac{E}{RT}\right) \quad (1)$$

where k represents the reaction rate constant, T stands for thermodynamic temperature (K), R is the universal gas constant (8.314 $J \cdot K^{-1} \cdot mol^{-1}$), E represents the activation energy ($kJ \cdot mol^{-1}$), and A is the pre-exponential factor (s^{-1}). The degradation rate of biomass can be expressed by Eq. 2,

$$\frac{d\alpha}{dt} = k(1-\alpha) \quad (2)$$

where $d\alpha/dt$ denotes the process rate, α is the fractional conversion and defined as $(w_0-w)/(w_0-w_f)$, and w_o, w_f, and w are the mass at the starting, end, and at a specific time t, respectively. Because temperature serves as the function of time, and it increases with an invariable heating rate β, the following equation can be derived.

$$T = \beta t + T_0 \quad (3)$$

Differentiation of the above correlativity results in Eq. 4.

$$dT = \beta dt \quad (4)$$

Eq. 2 can be expressed as follows in Eq. 5.

$$\frac{d\alpha}{1-\alpha} = \frac{k}{\beta} dT \quad (5)$$

The integration of Eq. 5 results in Eq. 6,

$$g(\alpha) = \frac{A}{\beta}\int_0^T \exp\left(-\frac{E}{RT}\right)dT \quad (6)$$

where $g(\alpha) = -\ln(1-\alpha)$.

Eq. 6 is integrated by the internal Coats-Redfern method to produce Eq. 7,

$$\ln\frac{g(\alpha)}{T^2} = \ln\left(\frac{AR}{\beta E}\left[1-\frac{2RT}{E}\right]\right) - \frac{E}{RT} \quad (7)$$

where $g(\alpha)$ represents the function of kinetic mechanism in an integral type.

The $2RT/E$ term is negligible because it is far less than 1. Thus, Eq. 7 is simplified to Eq. 8.

$$\ln\frac{g(\alpha)}{T^2} = \ln\frac{AR}{\beta E} - \frac{E}{RT} \quad (8)$$

For a given heating rate, the $\ln(g(\alpha)/T^2)$ term varies as $1/T$ with a slope of $-E/R$ linearly, and the intercept of the line corresponds to $\ln(AR/\beta E)$. Thus, pyrolysis kinetic parameters such as activation energy (E) and pre-exponential factor (A) in the main pyrolysis stage were calculated by the above equations.

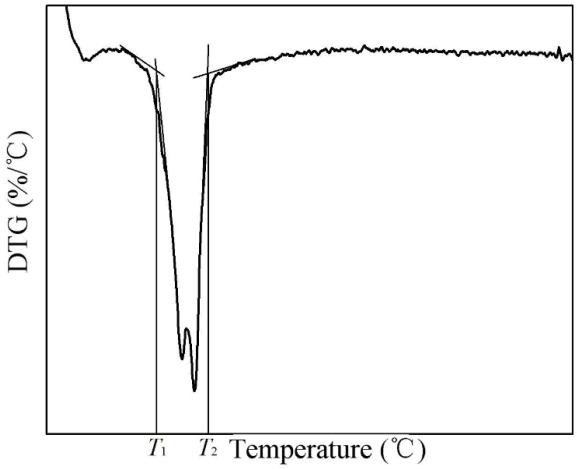

Fig. 1. DTG nomenclature for the studied temperature range

Here, it is important to note that the temperature points at which the temperatures were appointed are defined in Fig. 1, and the investigated temperature range is precisely between the named T_1 and T_2 (Yao *et al*. 2016c).

RESULTS AND DISCUSSION

Influence of Heating Rate on the Thermal Decomposition of CC Fractions

Figures 2(a)-(c) show the TG, DTG, and DSC curves, respectively, obtained for CC pyrolysis under different heating rates within the temperature range of 25 to 1200 °C. As shown by the TG curves in Fig. 2(a), CC pyrolysis followed stepwise mechanisms and mainly occurred in four steps that can be explained from its chemical composition. The first weight loss (below 140 °C) started at around 70 °C; it reflected the evaporation of

unbound moisture in biomass. As observed from the DTG curves in Fig. 2(b), the initial weight loss rates for all heating rates were quite slow, accompanied by a small shoulder peak within 70 to 140 °C. Munir *et al*. (2009) suggested that the weight loss occurring near 100 °C represents the initial degradation of lignin and hemicellulose components in biomass. Simultaneously, the DSC curves in Fig. 2(c) show an endothermic peak around 100 °C, indicating the energy adsorbed during the volatilization of moisture from CC.

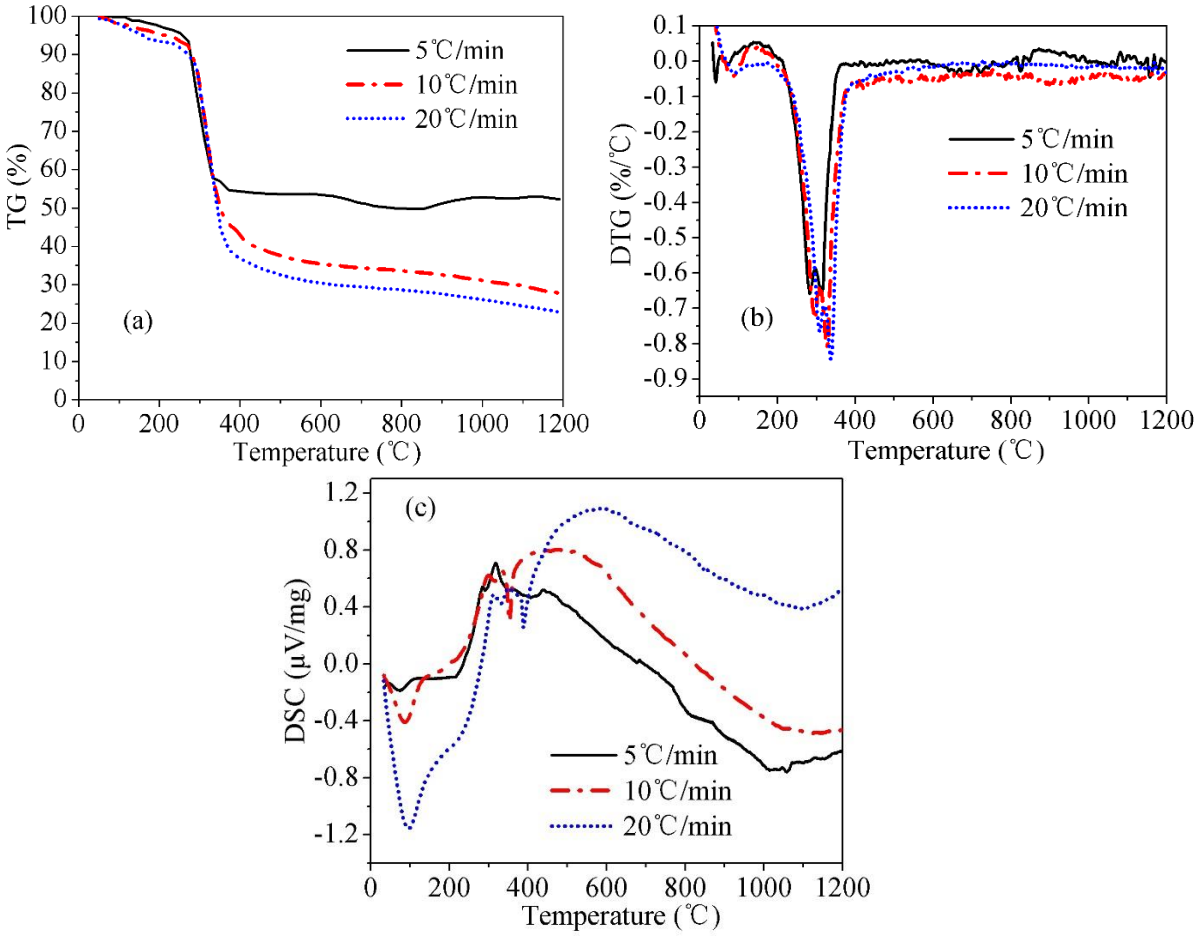

Fig. 2. Thermogram curves of CC under different heating rates (a) TG, (b) DTG, and (c) DSC

The second decomposition stage mainly took place from 140 °C to 420 °C, accompanied by two sharp peaks in the DTG curves. The weight loss in this pyrolysis zone made great contributions to the total weight loss (about 80 to 90 wt.%) during pyrolysis, and it was caused by the emission of volatiles from thermal degradation of the three fundamental components in biomass, namely cellulose, hemicellulose, and lignin. Cellulose, hemicellulose, and lignin decompose within 277 to 427 °C, 197 to 327 °C, and 277 °C to 527 °C, respectively (Du *et al*. 1990). The DTG curves show that the temperature relevant to the maximum weight loss rate tended to shift to a higher temperature zone as the heating rate was increased.

The third decomposition stage mainly occurred above 420 °C, and in this stage, the pyrolysis of CC proceeded at a relatively slower weight loss rate, which is mainly attributable to the decomposition of lignins at higher temperatures. After 600 °C, there was no significant weight loss, and the pyrolysis of CC was fundamentally complete.

The obtained TG and DTG data derived from TGA experiments are often used to establish thermal degradation profiles that clarify vital parameters. To evaluate the thermal performance of biomass more correctly, a comprehensive devolatilization parameter was proposed by Zeng *et al*. (2013) and is defined as follows,

$$D = \frac{(dw/dt)_{max}(dw/dt)_{mean}}{T_s T_{max} \Delta T_{1/2}} \quad (9)$$

where $(dw/dt)_{max}$ is the maximum weight loss rate, $(dw/dt)_{mean}$ is the mean weight loss rate, T_s is the starting temperature for volatile release and weight loss, T_{max} is the temperature of maximum weight loss rate, $\triangle T_{1/2}$ reflects the temperature of full width at half maximum for the main peak of DTG curves, and D reflects the volatile release index.

Table 2. Pyrolysis Feature Parameters of CC under Different Heating Rates

Heating rate (β) (°C/min)	Starting temperature (T_s) (°C)	Peak temperature (T_{max}) (°C)	Temperature of full width at half maximum ($\triangle T_{1/2}$) (°C)	Maximum weight loss rate $(dw/dt)_{max}$ (%/°C)	Mean weight loss rate $(dw/dt)_{mean}$ (%/°C)	Volatile release index (D) ($\times 10^{-8}$)	Total weight loss (W_t) (%)
5	176.7	314.8	71.4	-0.679	-0.098	1.68	47.79
10	179.8	326.5	67.5	-0.796	-0.139	2.79	69.65
20	183.3	334.4	69.2	-0.881	-0.148	3.07	77.23

Table 2 contains the characteristic parameters of starting temperature (T_s), peak temperature (T_{max}) of the main weight loss, along with the maximum degradation rate $(dw/dt)_{max}$ and the mean weight loss rate $(dw/dt)_{mean}$. All of these values increased remarkably with increased heating rate. The maximum degradation rate tended to rise at relatively faster heating rates. This effect was attributed to the fact that more thermal energy is released at faster heating rates, which promotes thermal transmission nearby and within CC (Baray *et al*. 2014). When the heating rate was 5, 10, and 20 °C/min, the total weight loss (W_t) was 47.79%, 69.65%, and 77.23%, respectively. Thus, CC pyrolysis at a higher heating rate resulted in a more complete decomposition.

Influence of Gas Flow on the Thermal Decomposition of CC Fractions

Figures 3(a)-(c) show the TG, DTG, and DSC curves, respectively, obtained for the thermal pyrolysis of CC fractions in different gas flow within the temperature range of 25 to 1200 °C. The main characteristic parameters determined from TG and DTG profiles for various gas flow cases are listed in Table 3.

Taken together, the TG curves in Fig. 3(a) and the results in Table 3 show that the total weight loss of CC increased slightly with increased gas flow, whereas the starting temperature of the pyrolysis decreased as the gas flow increased. Ferdous *et al*. (2001) demonstrated that carrier gas flow is closely related to the residence time of gaseous products released in the pyrolysis reaction zone. Hence, the residence time of the gaseous products decreased with elevated gas flow. These gaseous products released from the pyrolytic process could be pumped away the pyrolysis region in time by the elevated gas flow, and this could further accelerate the thermal cracking of biomass.

However, the influence of gas flow on the decomposition rate was not obvious, as observed from the DTG curves in Fig. 3(b). The DTG curves in different gas flow were almost completely overlapping. This phenomenon was consistent with the results in

Table 3; the peak temperature (T_{max}) corresponding to the maximum weight loss rate ($(dw/dt)_{max}$), the temperature of full width at half maximum ($\triangle T_{1/2}$), the mean weight loss rate ($(dw/dt)_{mean}$), and the volatile release index (D) showed little variation and association with the increase of gas flow.

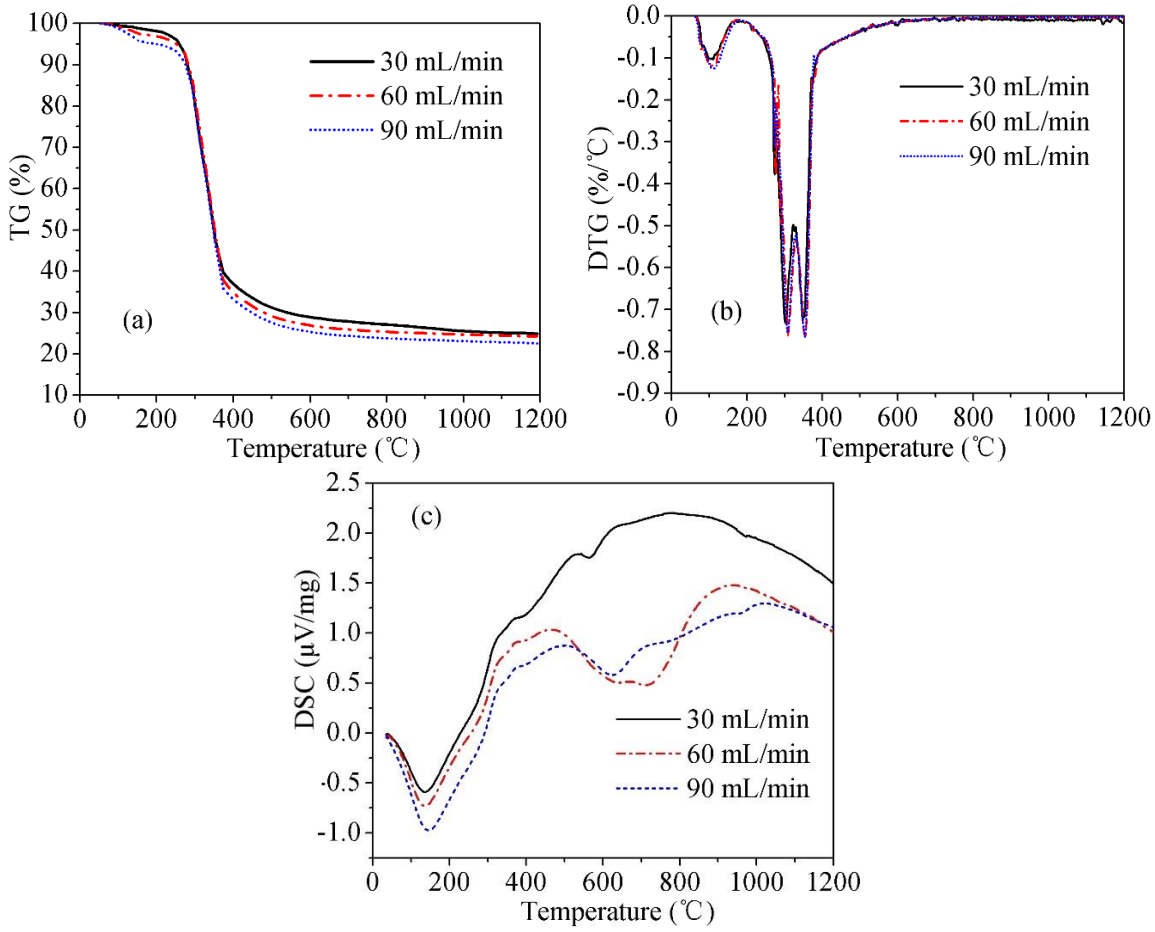

Fig. 3. Thermogram curves of CC in different gas flow (a) TG, (b) DTG, and (c) DSC curves

Table 3. Pyrolysis Feature Parameters of CC under Different Gas Flow

Gas flow (mL/min)	Starting temperature (T_s) (°C)	Peak temperature (T_{max}) (°C)	Temperature of full width at half maximum ($\triangle T_{1/2}$) (°C)	Maximum weight loss rate $(dw/dt)_{max}$ (%/°C)	Mean weight loss rate $(dw/dt)_{mean}$ (%/°C)	Volatile release index (D) ($\times 10^{-8}$)	Total weight loss (W_t) (%)
30	177.2	347.6	80.3	-0.73	-0.158	2.33	75.94
60	169.5	355.3	78.5	-0.77	-0.156	2.54	76.33
90	153.8	353.2	78.9	-0.77	-0.152	2.73	77.46

As shown in the DSC curves in Fig. 3(c), the strength of the endothermic peak caused by the volatilization of moisture within 100 to 200 °C was evidently enhanced by the relatively higher gas flow. With the increase of pyrolysis temperature, the heat of exothermic reactions during the pyrolysis increased gradually. Notably, the DSC curves in both cases of 60 and 90 mL/min presented evident endothermic peaks within the high

temperature zones (between 500 and 800 °C), while the DSC curve for case of 30 mL/min exhibited no obvious endothermic peak in this temperature zone, as it was primarily exothermic (Fig. 3(c)). This result suggested that when the gas flow increases, the carrier gas needs to absorb more heat and so further heats up the reaction temperature.

Influence of Particle Size on the Thermal Decomposition of CC Fractions

The CC particles of varying diameter ($d \leq 74$ μm, 74 μm < $d \leq 154$ μm, 154 μm < $d \leq 280$ μm, and 280 μm < $d \leq 450$ μm) were used to investigate the effects of particle size on thermal decomposition characteristics. The TG, DTG, and DSC results within 25 to 1200 °C for different particle sizes are shown in Figs. 4(a)-(c), respectively.

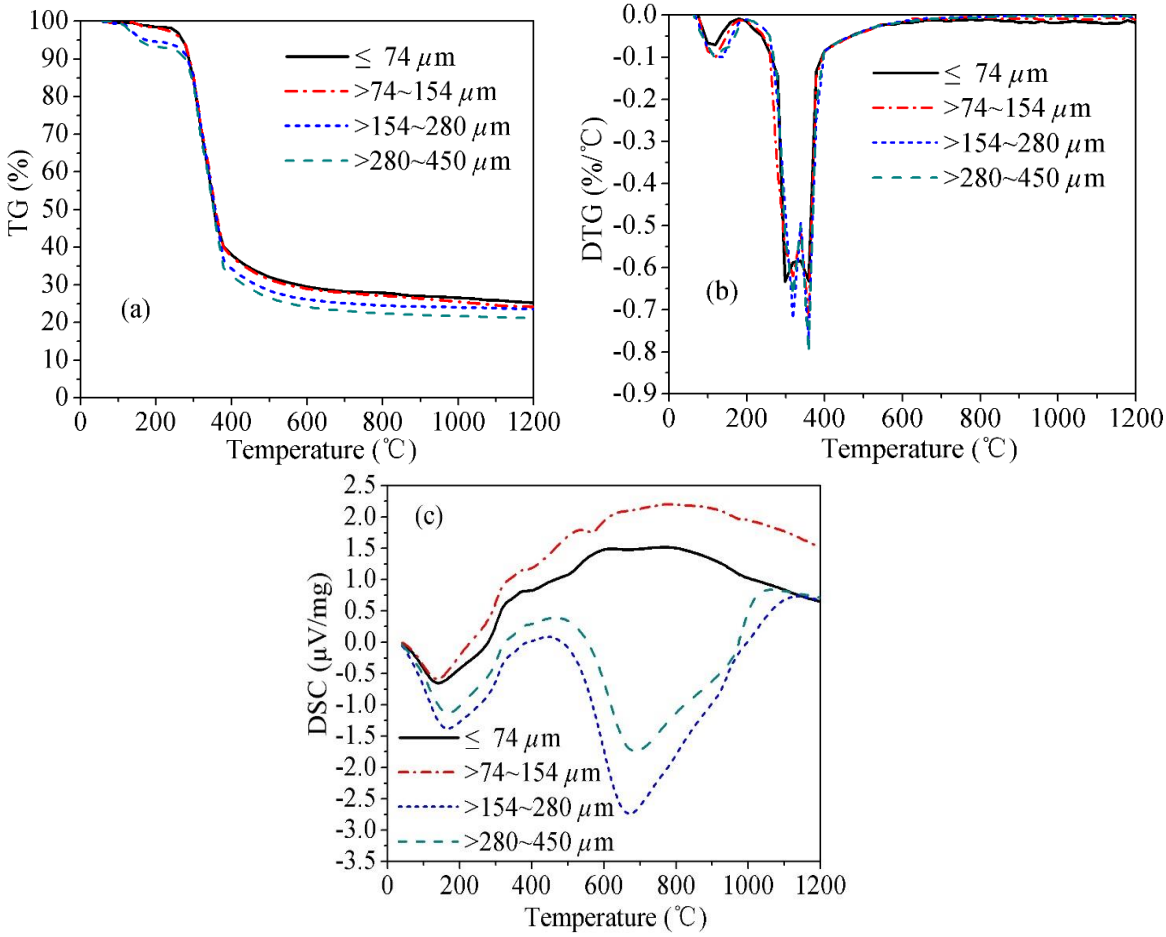

Fig. 4. Thermogram curves of CC particles of varying size (a) TG, (b) DTG, and (c) DSC

Generally speaking, the smaller particles have a relatively higher surface/volume ratio, which allows the primary pyrolysis fragments to escape more rapidly into the vapor. Thus, the centers of these smaller particles can reach the reactor temperature more rapidly than those of large particles (Zhang *et al*. 2007). In contrast, Figs. 4(a) and (b) clearly show that within the examined particle size range ($d \leq 450$ μm), the total weight loss and the peak weight loss rate for particles of $d \leq 74$ μm were the minimum. The particles between 280 and 450 μm in diameter were most easily pyrolyzed, followed by those with diameter between 154 and 280 μm, 74 < $d \leq 154$ μm, and $d \leq 74$ μm. These findings were confirmed by the characteristic parameters summarized in Table 4.

Given the bulk density of biomass powders and the heat-transfer limitations, these results and phenomena from the above analyses can be well explained. The bulk density of finer particles is larger than that of coarse particles. In general, larger particles have a smaller bulk density, and thus, the gaps in these particles are wider. Besides, as for the particles with large size, the gas diffusion resistance is much lower than that of particles with relatively smaller size, which is quite conductive to the diffusion of those gaseous products produced from the pyrolysis process. Moreover, during the thermal cracking process, increased biomass particle size favors the production of small-molecule gases, which further increased the total weight loss of biomass pyrolysis. Altogether, for the studied particles of $d \leq 450$ μm, the pyrolysis performance of larger particles was much better than that of small particles, and biomass feed particle size can significantly influence the thermal degradation of CC fractions.

Furthermore, Fig. 4(c) shows that the DSC for all particles in the tested size range could be divided into two categories based on the trend in DSC after 500 °C, which was similar for (1) the particles with a diameter smaller than 154 μm or (2) larger than 154 μm. For the particles of $d > 154$ μm, there was an evident and sharp endothermic peak within 500 to 800 °C, while there was no strong endothermic reaction for particles of $d \leq 154$ μm in this temperature stage. In contrast, their DSC curves reflected the general feature of exothermic reactions. According to Yang *et al*. (2007), the thermal degradation of hemicelluloses, celluloses, and lignin in biomass primarily occurs at 220 to 315 °C, 315 to 400 °C, and 160 to 900 °C, respectively. Thus, this variation tendency of heat flow within this higher temperature zone (500 to 800 °C) can be primarily ascribed to the thermal degradation of lignin components in CC.

Table 4. Pyrolysis Feature Parameters of CC Particles with Different Size

Particle size (μm)	Starting temperature (T_s) (°C)	Peak temperature (T_{max}) (°C)	Temperature of full width at half maximum ($\triangle T_{1/2}$) (°C)	Maximum weight loss rate $(dw/dt)_{max}$ (%/°C)	Mean weight loss rate $(dw/dt)_{mean}$ (%/°C)	Volatile release index (D) ($\times 10^{-8}$)	Total weight loss (W_t) (%)
≤74	182.5	352.6	85.6	-0.71	-0.153	1.97	75.01
>74~154	181.7	353.7	82.2	-0.73	-0.155	2.14	76.31
>154~280	179.6	355.3	80.5	-0.74	-0.156	2.25	77.47
>280~450	175.2	360.2	78.7	-0.81	-0.159	2.59	80.38

For smaller particles of $d \leq 154$ μm, the bulk density and specific surface area were relatively much larger than in large particles, which is much more advantageous to the heat transfer in pyrolysis. As a result, the heat released from the thermal degradation of celluloses and hemicelluloses in the early pyrolysis stage can basically provide the heat required for the degradation of the lignin components during the later pyrolysis stage. However, with respect to the larger particles of $154 \text{ μm} < d \leq 450$ μm, their bulk density and specific surface area were lower than those of small particles, and their heat conductive performance was not as good as that of finer particles. Thus, the pyrolytic process needs to absorb more heat to guarantee the continued pyrolysis of lignin components in the CC samples at higher temperatures.

Influence of Process Parameters on the Release of Bio-syngas Products from CC Pyrolysis

Pyrolysis of biomass can produce raw synthesis gas, which mainly contains CO, CO_2, CH_4, and H_2. The experimental gasification tests of CC waste conducted by Biagini *et al*. (2014) in a downdraft reactor at a demonstrative scale (nominal thermal throughput of 350 kW) suggested that the synthesis gas by CC pyrolysis was composed of 22.4-22.6% vol CO, 15.8-17.3% vol H_2, 11.3-12.3% vol CO_2, and 1.9-2.3% vol CH_4. Besides, in their study, they also found that the performance parameters (specific gas production 2 m^3/kg, syngas heating value 5.6 to 5.8 MJ/m^3) were comparable with those obtained with woody feedstock, which further indicates that the performance of CC in synthesis gas by pyrolysis mass can make great contribution to the syngas production in practice.

The evolution profiles of typical bio-syngas products (*i.e.*, CO, CO_2, CH_4, and H_2) during the pyrolytic process of CC samples under different process parameters were studied using the quantitative MS technique. The spectra for those gaseous products varied with the increase of temperature and are shown in Figs. 5 through 7. The evolution of bio-syngas compounds was in accordance with the DTG curves under different reaction parameters (Figs. 2(b), 3(b), and 4(b)).

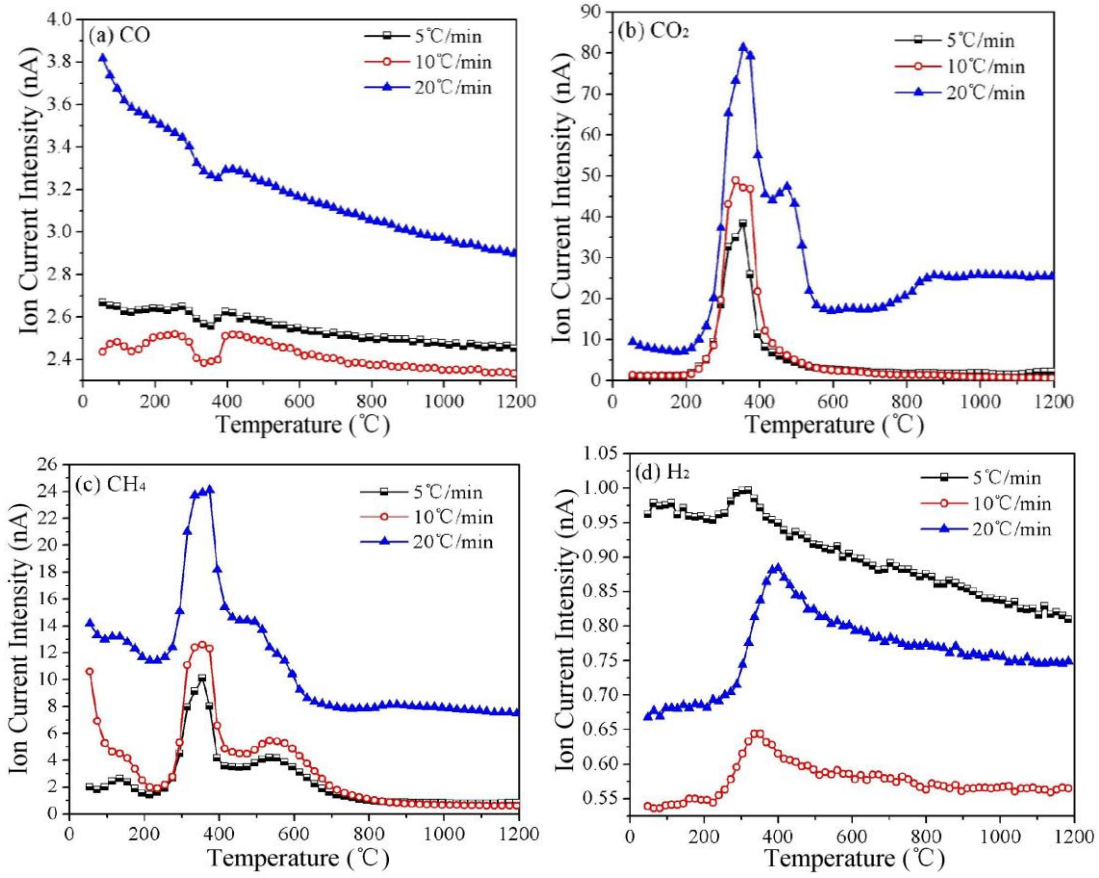

Fig. 5. Bio-syngas products varied with temperature under different heating rates

As shown in Figs. 5(a), 6(a), and 7(a), there were no obvious peaks of CO during pyrolysis. Meng *et al*. (2013) suggested that the CO was mainly was released from the cracking of carboxyl (C=O) and carbonyl (C–O–C) groups during the pyrolysis of

hemicelluloses and of lignins above 600 °C. Notably, the emission intensity of CO increased with increased heating rate and decreased with increased gas flow. There was no consistent decreasing or increasing trend for the CO evolution with increased biomass feed particle size. Thus, the thermal pyrolysis of CC fractions in a relatively lower gas flow and at a higher heating rate may be more suitable for the production of CO.

As can be observed in Figs. 5(b), 6(b), and 7(b), the shape of CO_2 emission fits well with the DTG curves below 400 °C, while the rest does not fit well with the DTG curves after 400 °C. CO_2 emission was mainly from the degradation of hemicelluloses, while CO was most likely generated from the pyrolysis of celluloses (Lv *et al*. 2012). The distinct emission of CO_2 appeared from 200 °C, and it reached a high peak intensity within 300 to 400 °C, which is the major pyrolysis zone of celluloses. The peak around 350 °C was ascribed to the decomposition of aromatic and aliphatic carboxyl groups in celluloses. Yang *et al*. (2007) suggested that below 500 °C, the abundant presence of C=O groups in hemicelluloses was favorable for CO_2 formation. As temperature increased, more stable ether structures and oxygen-bearing heterocycles in lignin are also decomposed into CO_2 (Wang *et al*. 2014). The variation in the evolution profiles of CO_2 (Figs. 5(b), 6(b), and 7(b)) as well as CH_4 (Figs. 5(c), 6(c), and 7(c)) with the change of heating rate and gas flow are similar to those of CO, implying that CO, CO_2, and CH_4 were the three main small-molecule gaseous products of pyrolysis.

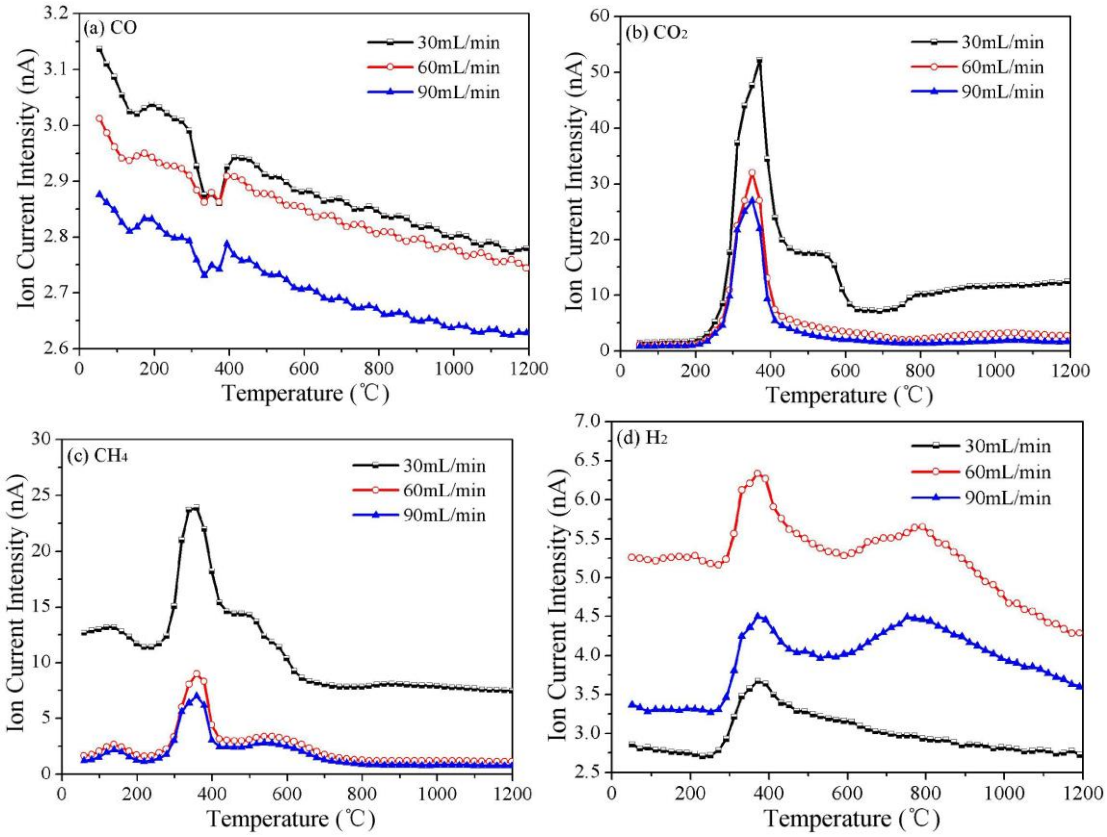

Fig. 6. Bio-syngas products varied with temperature under different gas flow

As observed from Figs. 5(c), 6(c), and 7(c), the shape of CH_4 emission curves under different parameters indicated that the release of CH_4 during the pyrolysis was

more complicated than the CO and CO_2 emissions. The highest concentration emission of CH_4 occurred at about 380 °C. As previously noted (Hodek *et al*. 1991; Arenillas *et al*. 2003), the CH_4 emission at relatively lower temperatures was most likely released from the C-C bond cleavage in aliphatic chains, whereas the CH_4 emission at higher temperature zones was mainly produced from the cracking of a weakly bonded methoxyl-O-CH_3 group as well as the break of having higher bond energy of methylene group -CH_2- (Ferdous *et al*. 2001). From the perspective of biomass components pyrolysis, the CH_4 was mainly released from the pyrolysis of lignin because it contains more methoxyl-O-CH_3 chemical groups than hemicelluloses and celluloses (Liu *et al*. 2008).

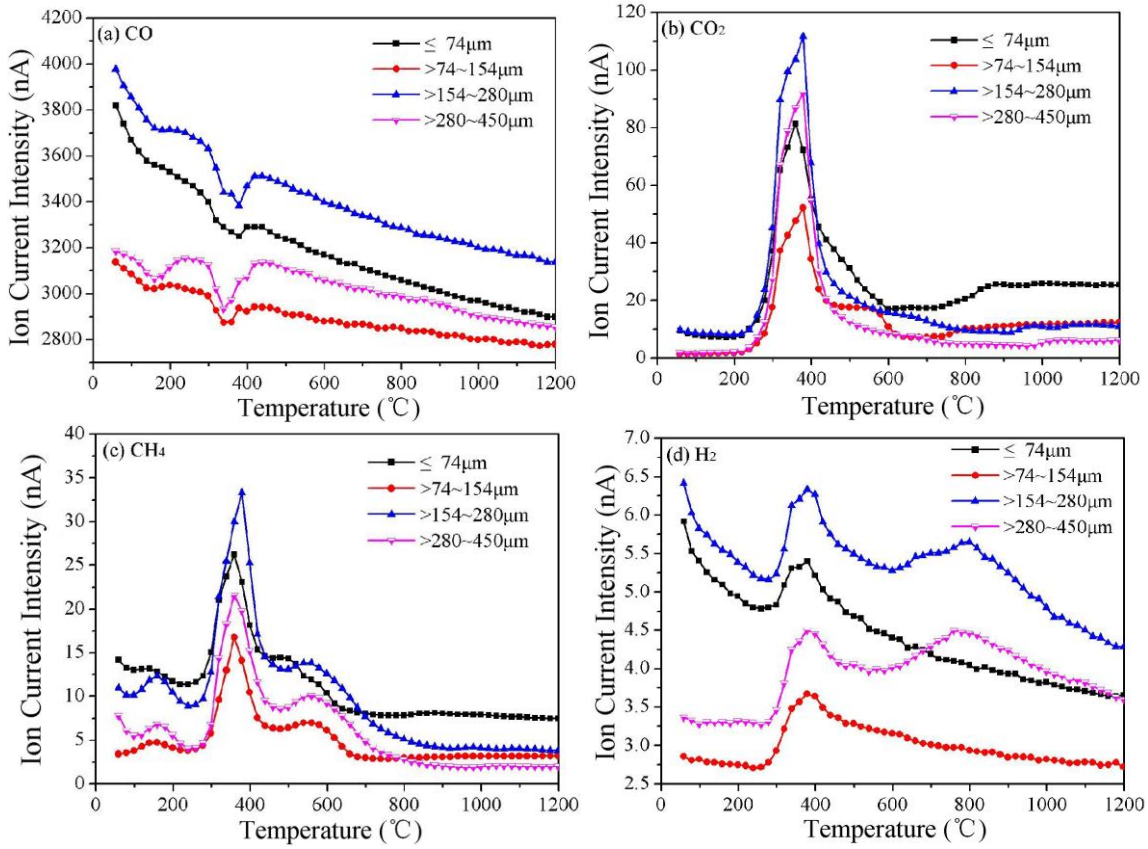

Fig. 7. Influence of particle size of CC on releasing characteristics of bio-syngas products

The emission of H_2 (Figs. 5(d), 6(d), and 7(d)) took place in a much broader temperature range compared with the other gases, which primarily occurred in two temperature stages. The first H_2 emission stage was from 200 to 500 °C, and in this period, the H_2 emission was mainly generated from the thermal degradation of celluloses and hemicelluloses (Wu *et al*. 2013). At the second stage beyond 500 °C, the curves of the evolved H_2 exhibited a decreasing trend under different heating rates (Fig. 5(d)), further revealing that the pyrolysis of lignin at relatively higher temperatures could also generate H_2. When the pyrolysis was carried out in various gas flows, especially for the cases of 60 and 90 mL/min (Fig. 6(d)), the emission of H_2 arrived at the second highest concentration peak at temperatures up to about 800 °C; this peak represented the thermal degradation of heterocyclic compounds or the condensation of aromatic and hydro-aromatic structures (Arenillas *et al*. 2003).

Furthermore, as shown in Fig. 5, the emission intensities of CO, CO_2, and CH_4 during CC pyrolysis at relatively faster heating rates were much higher than those values at low heating rates. H_2 emission showed the opposite effect, further indicating that the pyrolysis of CC at faster heating rates is more suitable for the production of bio-syngas products, especially for CO, CO_2, and CH_4. Figure 6 clearly shows the influence of gas flow on the release of these gaseous products, suggesting that the residence time of gas-phase products in the pyrolysis region was closely related to the gas flow. With increased gas flow, the emission intensities of CO, CO_2, and CH_4 decreased noticeably. Less residence time for volatiles released from the primary pyrolysis was needed to undergo secondary pyrolysis reactions, which further promoted the formation of small-molecule gases, especially CO and CH_4 (Jegers and Klein 1987). However, among these three cases (30, 60, and 90 mL/min), the H_2 emission intensity was the highest in the 60 mL/min gas flow. This result was consistent with the findings of Ferdous *et al*. (2001), who reported that the H_2 yield could be improved by reduced residence time when the yields of CO and CH_4 were decreased.

Figure 7 shows that the biomass feed particle size also had remarkable effects on the distribution of bio-syngas products, but the effects were not consistently changing. The maximum gas concentrations resulted from the pyrolysis of feed particles of 154 μm $< d \leq$ 280 μm, and the minimum concentrations resulted from the pyrolysis of particles of 74 μm $< d \leq$ 154 μm. Thus, in the examined ranges of heating rate, gas flow, and particle size, the pyrolysis of CC fractions with 154 μm $< d \leq$ 280 μm under the heating rate of 20 °C/min and in a gas flow of 30 to 60 mL/min was the most appropriate for the production of bio-syngas in industrial applications. In particular, as for the production of combustible gases (mainly including CO, CH_4, and H_2) in the synthesis gas product of the pyrolysis, the pyrolysis under the heating rate 20 °C/min and in a gas flow of 30 mL/min are the optimal for CO production and CH_4 production, while the pyrolysis under 5 °C/min and in a gas flow of 60 mL/min can be regarded as the optimal for H_2 production.

Influence of Different Process Parameters on Thermal Dynamics of CC

The TGA data obtained from experiments under different process parameters can be used for determining important kinetics and for investigating the effects of heating rate, gas flow, and biomass particle size on the thermal dynamics variation of CC. Based on the integral Coats-Redfern method, the linear variation between the $\ln(g(\alpha)/T^2)$ term and the slope of $-E/R$ (namely, $1/T$) under various thermolysis conditions was obtained. Figures 8(a), (b), and (c) show the variation between $\ln(g(\alpha)/T^2)$ and $1/T$ at different heating rates, gas flows, and particle sizes, respectively. As can be seen from Fig. 8, there was a good linear relationship between $\ln(g(\alpha)/T^2)$ and $1/T$.

The pyrolysis kinetic parameters in the main pyrolysis stage, such as the activation energy (E) and pre-exponential factor (A), were determined by these equations. The apparent activation energy, fitting equation, pre-exponential factor, and correlation between $\ln(g(\alpha)/T^2)$ and $1/T$ with different heating rates, gas flow, and particle sizes are summarized in Tables 5, 6, and 7, respectively. All these calculated values presented a good reproducibility with the standard deviation of less than 0.5%.

Tables 5 through 7 show the E values determined from the Coats-Redfern method under different process parameters varied from 64 to 80 $kJ \cdot mol^{-1}$, which was much lower than that of coal (generally 120 to 230 $kJ \cdot mol^{-1}$) recorded in the literature (Liang and Kozinski 2000). Besides, Wang *et al*. (2008) reported that the E values of sawdust calculated by distributed activation energy model (DAEM) ranged from 161.9 to 202.3

kJ/mol, and Yang *et al*. (2010) demonstrated that the *E* values of wheat straw calculated by the methods of Kissinger and Ozawa were respectively 103.92 and 107.69 kJ/mol, all of which are much higher than that of the studied CC samples. Thus, these results further indicate that CC can decompose more easily. Moreover, with increased heating rate and gas flow, the *E* values decreased gradually, revealing that the energy needed for the pyrolysis at a relatively faster heating rate or in a higher gas flow is certainly more than that of pyrolysis at a slower heating rate or in a lower gas flow.

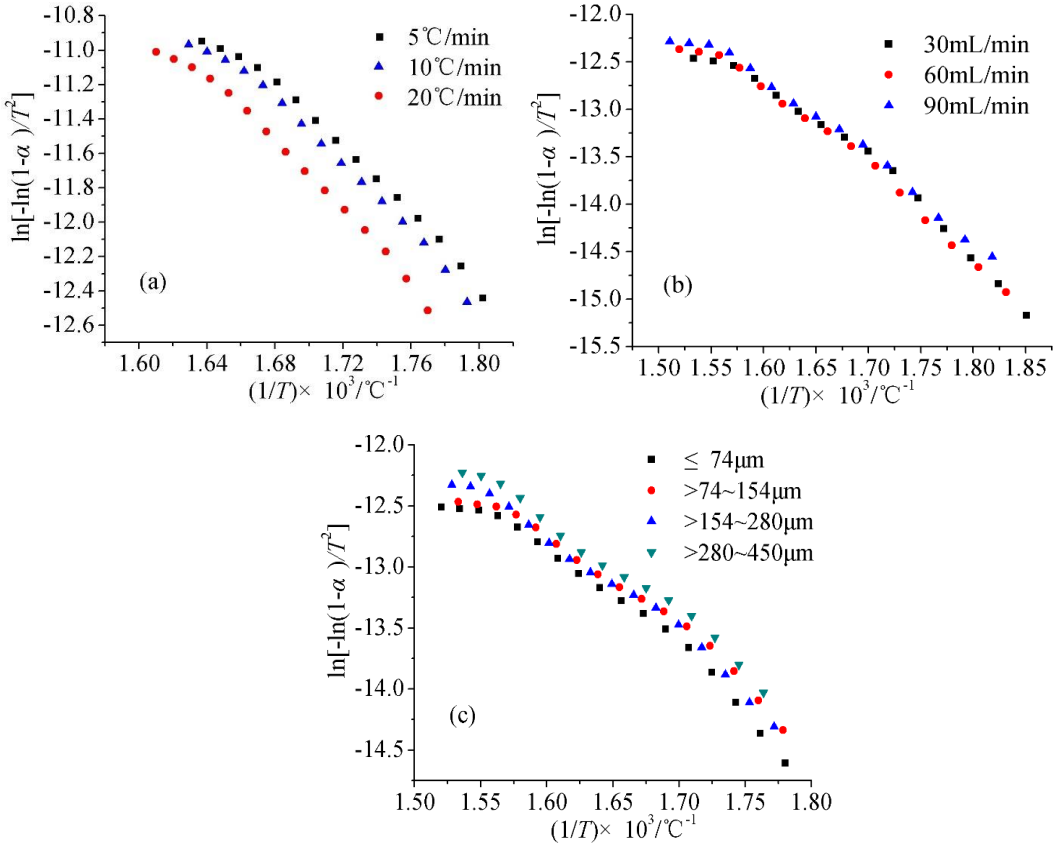

Fig. 8. The variation of correlation between the ln[g(*α*)/*T*^{2}] term and 1/*T* from Coats-Redfern method (a) at different heating rates, (b) in various gas flow, (c) for particles with different sizes

Table 5. Thermal Dynamics of CC Fractions under Different Heating Rates

Heating Rate (°C/min)	Temperature Range (°C)	Fitting Equation	*E* (kJ·mol^{-1})	*A* (s^{-1})	*R* (Correlation)
5	271-350	$Y = 4.4188-9.5116X$	79.08	4.518×10^4	0.99379
10	276-411	$Y = 4.1820-9.2288X$	76.73	1.316×10^5	0.99381
20	281-423	$Y = 4.0856-9.1148X$	75.78	2.015×10^5	0.99375

Table 6. Thermal Dynamics of CC Fractions in Different Gas Flow

Gas Flow (mL/min)	Temperature Range (°C)	Fitting Equation	*E* (kJ·mol^{-1})	*A* (s^{-1})	*R* (Correlation)
30	259-382	$Y = 1.0303-8.6297X$	71.73	2.417×10^2	0.98577
60	266-386	$Y = 0.8775-8.5606X$	71.17	2.059×10^2	0.99150
90	270-393	$Y = 0.2934-7.8485X$	65.25	1.052×10^2	0.99016

Table 7. Thermal Dynamics of CC Fractions with Varying Particle Size

CC Particle Size (μm)	Temperature Range (°C)	Fitting Equation	*E* (kJ·mol^{-1})	*A* (s^{-1})	*R* (Correlation)
≤74	285-383	$Y = 0.04829-8.0418X$	66.86	1.688×10^2	0.98235
>74~154	286-382	$Y = 0.7664-7.5168X$	62.49	3.235×10^2	0.98683
>154~280	287-384	$Y = 0.1564-8.0824X$	67.20	1.890×10^2	0.99231
>280~450	289-381	$Y = 0.2336-7.7513X$	64.44	1.958×10^2	0.99412

Table 7 shows that the biomass particle size had an evident effect on the thermal dynamics of CC, but the effect regularity was not obvious for different particle sizes. In addition, the linear correlations (*R*) relevant to the linear fittings under different thermolysis conditions were all greater than 0.98, suggesting a good linear dependence between $\ln(g(\alpha)/T^2)$ and $1/T$. This result further indicated that the pyrolytic process of CC fractions can be explained in terms of the first-order-reaction with the Arrhenius theory (Masgrau *et al*. 2003; Mangaraj *et al*. 2015).

CONCLUSIONS

1. TGA results showed evident differences in corncob (CC) pyrolysis under different conditions. Increasing the heating rate and gas flow promoted the thermal cracking of CC and further increased its weight loss. The activation energies determined from the Coats-Redfern method varied from 64 to 80 kJ·mol^{-1}. Particle size also had obvious effects on thermal dynamics, but the effect regularity was not clear on various levels of particle size.
2. In the examined particle size range ($d \leq 450$ μm), the pyrolysis behavior of larger CC particles was better than that of smaller particles. The pyrolysis of particles of $d > 154$ μm presented an endothermic peak within 500 to 800 °C, while the particles of $d \leq 154$ μm reflected the general feature of exothermic reactions in this temperature zone.
3. The evolution profiles of bio-syngas products corresponded well with thermogram curves. The emission intensities of CO, CO_2, and CH_4 increased with the increased heating rate, while they decreased with elevated gas flow. Using CC particles of 154 μm $< d \leq 280$ μm under 20 °C/min and in the gas flow of 30 to 60 mL/min resulted in the optimal bio-syngas production.

ACKNOWLEDGMENTS

The authors are very grateful for the support of Rural Energy Comprehensive Construction Fund of the Ministry of Agriculture of China (Grant. No. 2015-36).

REFERENCES CITED

Alshehri, S. M., Al-Fawaz, A., and Ahamad, T. (2013). "Thermal kinetic parameters and evolved gas analysis (TG-FTIR-MS) for thiourea-formaldehyde based polymer metal complexes," *Journal of Analytical and Applied Pyrolysis* 101, 215-221. DOI: 10.1016/j.jaap.2013.01.004

Arenillas, A., Rubiera, F., Pis, J. J., Cuesta, M. J., Iglesias, M. J., Jimenze, A., and Suarez-Ruiz, I. (2003). "Thermal behaviour during the pyrolysis of low rank perhydrous coals," *Journal of Analytical and Applied Pyrolysis* 68-69, 371-385. DOI: 10.1016/S0165-2370(03)00031-7

Arora, S., Kumar, M., and Dubey, G. P. (2009). "Thermal decomposition kinetics of rice husk: Activation energy with dynamic thermogravimetric analysis," *Journal of the Energy Institute* 82(3), 138-143. DOI: 10.1179/014426009X12448168550109

ASTM E1758-01 (2015). "Standard test method for determination of carbohydrates in biomass by high performance liquid chromatography," ASTM International, West Conshohocken, USA.

Ates, F., and Isikdag, M. A. (2009). "Influence of temperature and alumina catalyst on pyrolysis of corncob," *Fuel* 88(10), 1991-1997. DOI: 10.1016/j.fuel.2009.03.008

Baray, G. M. R., Silva, P. M. M., Melendez, Z. M., Gutierrez, J. S., Guzman, V. V., Lopez, O. A., and Collins-Martinez, V. (2014). "Thermogravimetric study on the pyrolysis kinetics of apple pomace as waste biomass," *International Journal of Hydrogen Energy* 39(29), 16619-16627. DOI: 10.1016/j.ijhydene.2014.06.012

Biagini, E., Barontini, F., and Tognotti, L. (2014). "Gasification of agricultural residues in a demonstrative plant: Corn cobs," *Bioresource Technology* 173, 110-116. DOI: 10.1016/j.biortech.2014.09.086

Cao, Q., Xie, K. C., Bao, W. R., and Shen, S. G. (2004). "Pyrolytic behavior of waste corn cob," *Bioresource Technology* 94(1), 83-89. DOI: 10.1016/j.biortech.2003.10.031

Czernik, S., and Bridgwater, A. V. (2004). "Overview of applications of biomass fast pyrolysis oil," *Energy and Fuels* 18(2), 590-598. DOI: 10.1021/ef034067u

Du, Z. Y., Sarofim, A. F., and Longwell, J. P. (1990). "Activation energy distribution in temperature-programmed desorption: Modeling and application to the soot oxygen system," *Energy Fuels* 4(3), 296-302. DOI: 10.1021/ef00021a014

Duman, G., Okutucu, C., Ucar, S., Stahl, R., and Yanik, J. (2011). "The slow and fast pyrolysis of cherry seed," *Bioresource Technology* 102(2), 1869-1878. DOI: 10.1016/j.biortech.2010.07.051

Feng, J., YuHong, Q., and Green, A. C. S. (2006). "Analytical model of corn cob Pyroprobe-FTIR data," *Biomass and Bioenergy* 30(5), 486-492. DOI: 10.1016/j.biombioe.2005.09.004

Ferdous, D., Dalai, A. K., Bej, S. K., Thring, R. W., Bakhshi, N. N. (2001). "Production of H_2 and medium btu gas *via* pyrolysis of lignins in a fixed-bed reactor," *Fuel Processing Technology* 70(1), 9-26. DOI: 10.1016/S0378-3820(00)00147-8

Gai, C., Dong, Y. P., and Zhang, T. H. (2013). "The kinetic analysis of the pyrolysis of agricultural residue under non-isothermal conditions," *Bioresource Technology* 127, 298-305. DOI: 10.1016/j.biortech.2012.09.089

GB/T 28731-2012 (2012). "Proximate analysis of solid biofuels," Standardization Administration of China, Beijing, China.

Hodek, W., Kirschstein, J., and Van Heek, K. H. (1991). "Reactions of oxygen containing structures in coal pyrolysis," *Fuel* 70(3), 424-428. DOI: 10.1016/0016-2361(91)90133-U

Ioannidou, O., Zabaniotou, A., Antonakou, E. V., Papazisi, K. M., Lappas, A. A., and Athanassiou, C. (2009). "Investigating the potential for energy, fuel, materials and chemicals producing from corn residues (cobs and stalks) by non-catalytic and catalytic pyrolysis in two reactor configurations," *Renewable and Sustainable Energy Reviews* 13(4), 750-762. DOI: 10.1016/j.rser.2008.01.004

Jegers, H. E., and Klein, M. T. (1987). "Primary and secondary lignin pyrolysis reaction pathways," *Industrial & Engineering Chemistry Process Design and Development* 24(1), 173-183. DOI: 10.1021/i200028a030

Lanzetta, M., and Di Blasi, C. (1998). "Pyrolysis kinetics of wheat and corn straw," *Journal of Analytical and Applied Pyrolysis* 44(2), 181-192. DOI: 10.1016/S0165-2370(97)00079-X

Liang, X. H., and Kozinski, J. A. (2000). "Numerical modeling of combustion and pyrolysis of cellulosic biomass in thermogravimetric systems," *Fuel* 79(12), 1477-1486. DOI: 10.1016/S0016-2361(99)00286-0

Liu, Q., Wang, S. R., Zheng, Y., Luo, Z. Y., and Cen, K. F. (2008). "Mechanism study of wood lignin pyrolysis by using TG-FTIR analysis," *Journal of Analytical and Applied Pyrolysis* 82(1), 170-177. DOI: 10.1016/j.jaap.2008.03.007

Liu, X., Zhang, Y., Li, Z. F., Feng, R., and Zhang, Y. Z. (2014). "Characterization of corncob-derived biochar and pyrolysis kinetics in comparison with corn stalk and sawdust," *Bioresource Technology* 170, 76-82. DOI: 10.1016/j.biortech.2014.07.077

Lv, G. J., and Wu, S. B. (2012). "Analytical pyrolysis studies of corn stalk and its three main components by TG-MS and Py-GC/MS," *Journal of Analytical and Applied Pyrolysis* 97, 11-18. DOI: 10.1016/j.jaap.2012.04.010

Mangaraj, S., Goswami, T. K., and Mahajan, P. V. (2015). "Development and validation of a comprehensive model for map of fruits based on enzyme kinetics theory and Arrhenius relation," *Journal of Food Science and Technology* 52(7), 4286-4295. DOI: 10.1007/s13197-014-1364-0

Masgrau, L., Gonzalez-Lafont, A., and Lluch, J. M. (2003). "The curvature of the Arrhenius plots predicted by conventional canonical transition-state theory in the absence of tunneling," *Theoretical Chemistry Accounts* 110(5), 352-357. DOI: 10.1007/s00214-003-0484-9

Mazlan, M. A. F., Uemura, Y., Osman, N. B., and Yusup, S. (2015). "Fast pyrolysis of hardwood residues using a fixed bed drop-type pyrolyzer," *Energy Conversion and Management* 98, 208-214. DOI: 10.1016/j.enconman.2015.03.102

Meng, A. H., Zhou, H., Qin, L., Zhang, Y. G., and Li, Q. H. (2013). "Quantitative and kinetic TG-FTIR investigation on three kinds of biomass pyrolysis," *Journal of Analytical and Applied Pyrolysis* 104, 28-37. DOI: 10.1016/j.jaap.2013.09.013

Miura, T., and Maki, T. (1998). "A simple method for estimating $f(E)$ and $k_0(E)$ in the distributed activation energy model," *Energy and Fuels* 12(5), 864-869. DOI: 10.1021/ef970212q

Mohan, D., Charles, J., Pittman, U., and Steele, P. H. (2006). "Pyrolysis of wood/biomass for bio-oil: A critical review," *Energy and Fuels* 20(3), 848-889. DOI: 10.1021/ef0502397

Munir, S., Daood, S. S., Nimmo, W., Cunliffe, A. M., and Gibbs, B. M. (2009). "Thermal analysis and devolatilization kinetics of cotton stalk, sugar cane bagasse and shea meal under nitrogen and air atmospheres," *Bioresource Technology* 100(3), 1413-1418. DOI: 10.1016/j.biortech.2008.07.065

Pittman, C. U., Mohan, D., Eseyin, A., Li, Q., Ingram, L., Hassan, E. B. M., Mitchell, B., Guo, H., and Steele, P. H. (2012). "Characterization of bio-oils produced from fast pyrolysis of corn stalks in an auger reactor," *Energy and Fuels* 26(6), 3816-3825. DOI: 10.1021/ef3003922

Rath, J., and Staudinger, G. (2001). "Cracking reactions of tar from pyrolysis of spruce wood," *Fuel* 80(10), 1379-1389. DOI: 10.1016/S0016-2361(01)00016-3

Shen, D. K., Ye, J. M., Xiao, R., and Zhang, H. Y. (2013). "TG-MS analysis for thermal decomposition of cellulose under different atmospheres," *Carbohydrate Polymers* 98(1), 514-521. DOI: 10.1016/j.carbpol.2013.06.031

Singh, S., Wu, C. F., and Williams, P. T. (2012). "Pyrolysis of waste materials using TGA-MS and TGA-FTIR as complementary characterisation techniques," *Journal of Analytical and Applied Pyrolysis* 94, 99-107. DOI: 10.1016/j.jaap.2011.11.011

Sun, Z. A., Shen, J. Z., Jin, B. S., and Wei, L. Y. (2010). "Combustion characteristics of cotton stalk in FBC," *Biomass and Bioenergy* 34(5), 761-770. DOI: 10.1016/j.biombioe.2010.01.019

Trninic, M., Wang, L., Varhegyi, G., Gronli, M., and Skreiberg, O. (2012). "Kinetics of corncob pyrolysis," *Energy and Fuels* 26(4), 2005-2013. DOI: 10.1021/ef3002668

Vamvuka, D., Kakaras, E., Kastanaki, E., and Grammelis, P. (2003). "Pyrolysis characteristics and kinetics of biomass residuals mixtures with lignite," *Fuel* 82(15-17), 1949-1960. DOI: 10.1016/S0016-2361(03)00153-4

Wang, G., Li, W., Li, B. Q., and Chen, H. K. (2008). "TG study on pyrolysis of biomass and its three components under syngas," *Fuel* 87(4-5), 552-558. DOI: 10.1016/j.fuel.2007.02.032

Wang, T. P., Yin, J., Liu, Y., Lu, Q., and Zheng, Z. M. (2014). "Effects of chemical inhomogeneity on pyrolysis behaviors of corn stalk fractions," *Fuel* 129, 111-115. DOI: 10.1016/j.fuel.2014.03.061

Worasuwannarak, N., Sonobe, T., and Tanthapanichakoon, W. (2007). "Pyrolysis behaviors of rice straw, rice husk, and corncob by TG-MS technique," *Journal of Analytical and Applied Pyrolysis* 78(2), 265-271. DOI: 10.1016/j.jaap.2006.08.002

Wu, C. F., Wang, Z. C., Huang, J., and Williams, P. T. (2013). "Pyrolysis/gasification of cellulose, hemicellulose and lignin for hydrogen production in the presence of various nickel-based catalysts," *Fuel* 106, 697-706. DOI: 10.1016/j.fuel.2012.10.064

Xu, R., Ferrante, L., Briens, C., and Berruti, F. (2009). "Flash pyrolysis of grape residues into biofuel in a bubbling fluid bed," *Journal of Analytical and Applied Pyrolysis* 86(1), 58-65. DOI: 10.1016/j.jaap.2009.04.005

Yang, H. P., Yan, R., Chen H. P., Lee, D. H., and Zheng, C. G. (2007). "Characteristics of hemicellulose, cellulose and lignin pyrolysis," *Fuel* 86(12), 1781-1788. DOI: 10.1016/j.fuel.2006.12.013

Yang, Q., Wu, S. B., Lou, R., and Lv, G. J. (2010). "Analysis of wheat straw lignin by thermogravimetry and pyrolysis-gas chromatography/mass spectrometry," *Journal of Analytical and Applied Pyrolysis* 87(1), 65-69. DOI: 10.1016/j.jaap.2009.10.006

Yao, X. W., Xu, K. L., and Liang, Y. (2016a). "Comparing the thermo-physical properties of rice husk and rice straw as feedstock for thermochemical conversion and characterization of their waste ashes from combustion," *BioResources* 11(4), 10549-10564. DOI: 10.15376/biores.11.4.10549-10564

Yao, X. W., Xu, K. L., and Li, Y. (2016b). "Physicochemical properties and possible applications of waste corncob fly ash from biomass gasification industries of china," *BioResources* 11(2), 3783-3798. DOI: 10.15376/biores.11.2.3783-3798

Yao, X. W., Xu, K. L., and Liang, Y. (2016c). "Research on the thermo-physical properties of corncob residues as gasification feedstock and assessment for characterization of corncob ash from gasification," *BioResources* 11(4), 9823-9841. DOI: 10.15376/biores.11.4.9823-9841

Zhang, J. L., Toghiani, H., Mohan, D., Pittman, C. U., and Toghiani, R. K. (2007). "Product analysis and thermodynamic simulations from the pyrolysis of several biomass feedstocks," *Energy and Fuels* 21(4), 2373-2385. DOI: 10.1021/ef0606557

Zhang, H. Y., Xiao, R., Huang, H., and Xiao, G. (2009). "Comparison of non-catalytic and catalytic fast pyrolysis of corncob in a fluidized bed reactor," *Bioresource Technology* 100(3), 1428-1434. DOI: 10.1016/j.biorrech.2008.08.031

Zeng, W. Y., Jin, J., Zhang, H., Gao, W. J., Gao, X. Y., Dong, Z., and Meng, L. (2013). "Pyrolysis characteristics and kinetics mechanism of two typical sludge," *Journal of Combustion Science and Technology* 19(6), 544-548. DOI: 10.11715/rskxjs.R201303020

Article submitted: December 16, 2016; Peer review completed: February 3, 2017; Revised version received and accepted: February 17, 2017; Published: February 22, 2017.
DOI: 10.15376/biores.12.2.2748-2767